Available online at www.sciencedirect.com
ScienceDirect
Journal of Power Sources 161 (2006) 225–231
JOURNAL OF POWER SOURCES
www.elsevier.com/locate/jpowsour

Mass transfer in graded microstructure solid oxide fuel cell electrodes

Eric S. Greene [a], Wilson K.S. Chiu [a,*], Maria G. Medeiros [b]

[a] *Department of Mechanical Engineering, University of Connecticut, 191 Auditorium Rd. Storrs, CT 06269-3139, USA*
[b] *Naval Undersea Warfare Center, Division Newport, 1176 Howell St. Newport, RI 02841, USA*

Received 8 February 2006; received in revised form 26 March 2006; accepted 28 March 2006
Available online 15 May 2006

Abstract

A computational model is presented in which performance of a solid oxide fuel cell with functionally graded electrodes can be predicted. The model calculates operational cell voltages at varying electrode porosity and operational parameters, accounting for losses from mass transport through the porous electrodes, ohmic losses from current flow through the electrodes and electrolyte, and activation polarization. Specifically the physical phenomena that occur when the electrode is designed with a change in microstructure along its thickness are studied. Cell polarizations are investigated to find arrangements for which the minimal polarization occurs. Both diluted hydrogen fuel and partially reformed methane streams with internal reforming are investigated. It is concluded that performance benefits are seen when the electrodes are given an increase in porosity near the electrolyte interface for certain fuels and with satisfactory material properties. Enhanced reformation is observed in high tortuosity structures due to increased gas residence time within the electrode.

Keywords: Solid oxide fuel cell; Functionally graded microstructure; Multi-component mass transfer; Mass transfer modeling

1. Introduction

The fuel flexibility of solid oxide fuel cell (SOFC) systems has lead to their development as next generation power sources. The direct use of liquid fuels in a single cell has been demonstrated [1]. The inherent high volumetric energy density of hydrocarbon and particularly liquid fuels leads to theoretical increases in total system power density. They are therefore well suited to a volume limited design constraint such as air independent undersea vehicles and other applications. Consideration of the effect that this has on the performance and design of SOFC systems is important.

Functional grading of SOFC components, including the electrodes and electrolyte, has been applied in many successful ways. The purpose of this can be to increase electrochemical activity and to optimize the cell performance [1–4], separate chemically reactive components [3,5], create an interface between two layers incompatible because of thermal expansion [6], and to increase mechanical stability [7]. Modeling of the graded electrode manufacturing process has also been carried out to gain physical insight into the graded electrode creation process [8,9]. It is interesting to note that there have been limited studies into modeling the mass transfer effects of electrode microstructural changes during cell performance. This paper addresses the mass transfer effects present in the porous SOFC electrodes with graded microstructure.

This study addresses modeling the performance of a single solid oxide fuel cell operating on partially reformed methane or diluted hydrogen fuel. It is composed of an anode, electrolyte, and cathode assembly. The model is able to calculate voltage loss and species concentration, mass flux, and chemical reaction rate profiles. This is achieved by including the electrochemical reactions at the anode/electrolyte and the cathode/electrolyte interfaces, internal steam reforming kinetics, electric and ionic ohmic losses, and multicomponent mass transfer in the porous electrodes. This 1D model is suited for studying the details of the phenomena that occur in the fuel cell under operating conditions. Specifically, the changes that occur to cell polarization and gas concentration distribution will be studied to obtain physical insight and performance characteristics from microstructural features that are both linearly changing with depth and constant throughout the entire electrode thickness.

* Corresponding author. Tel.: +1 860 486 3647; fax: +1 860 486 5088.
E-mail address: wchiu@engr.uconn.edu (W.K.S. Chiu).

0378-7753/$ – see front matter © 2006 Elsevier B.V. All rights reserved.
doi:10.1016/j.jpowsour.2006.03.063

Nomenclature

B_i	Effective permeability coefficient of species i ($m^2\ s^{-1}$)
c_i, c_t	Concentration of species i, total concentration ($mol\ m^{-3}$)
d	thickness (μm)
D^k	Gas diffusion constant ($m^2\ s^{-1}$)
E, E^0	Fuel cell electrochemical potential, theoretical maximum fuel cell electrochemical potential (V)
F	Faraday's constant, 96,485 (C)
i	Current density ($A\ cm^{-2}$)
i_o	Exchange current density ($A\ cm^{-2}$)
K	Knudsen number (=λ/2r)
L	Thickness of layer (μm)
N_i	Molar flux rate of species i ($mol\ m^{-2}\ s$)
p	Pressure (atm.)
p_i	Partial pressure of gas (atm.)
R	Universal gas constant, 8.314 ($J\ K\text{-}mol^{-1}$)
$\langle r \rangle$	Mean pore diameter (μm)
$\langle r^2 \rangle$	Statistical distribution parameter of pore size around mean (μm^2)
T	Temperature (K)
y_i	Concentration percentage of component i

Greek letters

ε	Porosity of material
η	Gas mixture viscosity ($m^2\ s^{-1}$)
η_{act}	Activation polarization (V)
η_{conc}	Concentration polarization (V)
η_{ohm}	Ohmic polarization (V)
λ	Mean free path length (m)
ρ	Electrical resistivity (Ω*m)
τ	Tortuosity of porous material
ψ	Ratio of porosity to tortuosity (ε/τ)

Subscripts

A	Anode
C	Cathode
E	Electrolyte
i,j	Component identifier

Superscripts

d	Diffusion
k	Knudsen
m	Molecular
op	Operational
sup	Supply
TPB	Triple phase boundary
p	Permeation

2. Technical approach

A schematic of this SOFC model is shown in Fig. 1. The main goal of the model is to calculate the voltage of a cell at a prescribed current draw as measured from the surface of the anode to the surface of the cathode for various electrode microstructures. A 1D model for predicting solid oxide fuel cell performance is presented which will allow modeling of most relevant phenomena.

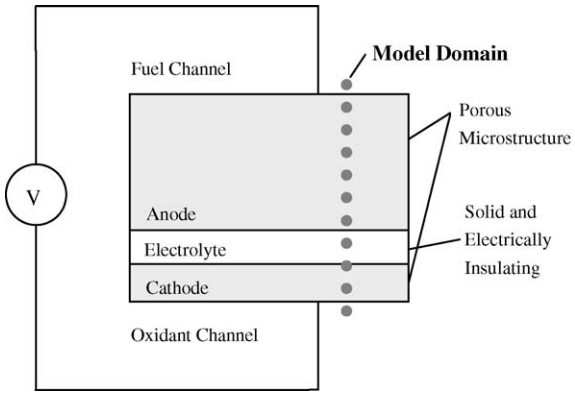

Fig. 1. Schematic of the computational model domain and geometry of a SOFC.

The expression for the operating voltage of the cell is calculated according to:

$$E_{op} = E - \eta_{act} - \eta_{ohm} - \eta_{conc} \quad (1)$$

In Eq. (1), E_{op} is the operational fuel cell voltage, E is the ideal Nernst voltage calculated from thermodynamic principles, η_{ohm} is the overpotential caused by electronic and ionic ohmic losses from current flowing through the fuel cell materials, and η_{conc} is the voltage loss caused by reduced fuel and oxidant concentrations. These are all highly dependent on current density.

The Nernst voltage can be calculated for a H_2/O_2 fuel cell by:

$$E = E^0 + \frac{RT}{2F} \ln \frac{p_{H_2} {p_{O_2}}^{0.5}}{p_{H_2O}} \quad (2)$$

The thermodynamically maximum voltage obtainable for a given temperature (E^0) is calculated according to Eq. (3), which utilizes the Gibbs free energy difference (ΔG°) between fuel cell products and reactants, where $n = 2$ is the number of equivalent electrons per mole reacted. The electrochemical oxidation of CO is assumed to be negligible because it is entirely consumed in the reforming reactions of the cell.

$$E^0 = \frac{-\Delta G^\circ}{nF} \quad (3)$$

The activation overpotential can be accurately modeled by the Butler-Volmer equation for a fuel cell [10]:

$$i = i_o \left\{ \exp\left(\beta \frac{2F\eta_{act}}{RT}\right) - \exp\left(-(1-\beta)\frac{2F\eta_{act}}{RT}\right) \right\} \quad (4)$$

This equation includes the exchange current density i_o found through experiments and the transfer coefficient β that is determined through correlation with well controlled experiments. This study assumes that functional grading of electrodes, which occurs in the bulk material, does not change the amount of electrochemically active sites at the triple phase boundary (TPB).

The ohmic losses through the cell components, η_{ohm}, are found by using Ohm's law. The voltage drop is proportional

to the current by $\eta_{\text{ohm},x} = iR$ where the resistance, R, is the product of the material's effective resistivity, ρ, and the thickness of the layer, L. For porous materials the local effective resistivity is:

$$\rho = \frac{\rho_{\text{bulk}}}{1-\varepsilon} \tag{5}$$

The total effective resistivity of an electrode is calculated by finding the average porosity value for a structure and applying Eq. (5). The total ohmic loss is then the sum of the three component losses from the anode, cathode, and electrolyte.

The concentration polarization occurs due to reduced reactant concentration at the electrochemically active regions. Many situations can lead to significant resistance to mass transfer through the porous electrodes. This causes a concentration gradient of products and reactants across the electrode that leads to lower concentrations of reactants at the triple phase boundary where reactants are used. A dense layer of electrode is needed at the TPB. This is critical to increase the length of the boundary between the electrode, electrolyte, and the gas phase, increase the electrochemical activity of the cell, and therefore enhance performance. It is an assumption of the model that the thickness of the layer needed to provide the enhanced electrochemical activity was much thinner than the anode thickness used for support and therefore has a negligible effect on the mass transfer characteristics.

The concentration polarization, η_{conc}, is the difference in Nernst potential between the reactant supply channel, E^{sup}, and the triple phase boundary, E^{TPB} [11].

$$\eta_{\text{conc}} = E^{\text{sup}} - E^{\text{TPB}} \tag{6}$$

Modeling mass transport in the electrodes is essential to obtaining the necessary concentrations for calculating the concentration polarization. The mean transport pore model (MTPM) [12,13] is used to approximate the geometry of a porous media as continuous round pores from the electrode surface to the interface with the electrolyte. The relevant details are given below. Within the framework of the MTPM, the electrode geometry is described by three parameters Ψ, $\langle r\rangle$, and $\langle r^2\rangle$.

The parameter Ψ can be thought of as a measure of the "effective" porosity of the material. It adjusts the real porosity for the extra resistance that the tortuous path imposes to the flow of gasses. Knudsen diffusion must be taken into account in the calculations because the pore sizes are on the same order of magnitude as the mean free path length of the gasses. The total mass transport is given by:

$$N_i = N_i^{\text{d}} + N_i^{\text{p}} \tag{7}$$

where N_i^{d} is the total component diffusion flux and N_i^{p} is the total component permeation flux. This equation also takes into account Knudsen diffusion:

$$\frac{N_i^{\text{d}}}{D_i^{\text{k}}} + \sum_{\substack{j=1\\ j\neq i}}^{n} \frac{y_j N_i^{\text{d}} - y_i N_j^{\text{d}}}{D_{ij}^{\text{m}}} = -c_{\text{T}} \frac{\text{d}y_i}{\text{d}x} \tag{8}$$

Total component flux can be described by the equation:

$$N_i^{\text{p}} = -y_i B_i \frac{\text{d}c_{\text{T}}}{\text{d}x}, \quad i = 1,\ldots,n \tag{9}$$

$$B_i = K_i \Psi \langle r\rangle \phi + \omega K_i \Psi \langle r\rangle (1-\phi) + \frac{\langle r^2\rangle \Psi p}{8\eta} i = 1, n \tag{10}$$

$$\phi^{-1} = 1 + \left(\frac{\lambda}{2\langle r\rangle}\right)^{-1} \tag{11}$$

In the above equations K_i is the Knudsen number of component i, ω is a physical factor that depends on the Knudsen wall slip, and ν_i is the square root of the relative molecular weights. Properties and values for gasses used in this study are available in literature [14].

The model takes into account the chemical kinetics of both the steam reforming and the shift reaction described in Eqs. (12) and (13).

$$CH_4 + H_2O \Leftrightarrow 3H_2 + CO \tag{12}$$

$$CO + H_2O \Leftrightarrow H_2 + CO_2 \tag{13}$$

These rates are determined experimentally for the general temperature and pressure found within the anode being modeled [12,13]. In order to have a simple representation, they are described by a quasi-homogeneous expression. The rates of reaction of the steam reforming and the shift reactions are described by Eqs. (14) and (15), respectively.

$$R_{\text{r}} = {k_{\text{r}}}^{+} p_1 p_3 - {k_{\text{r}}}^{-} p_2 (p_4)^3 \tag{14}$$

$$R_{\text{s}} = {k_{\text{s}}}^{+} p_2 p_3 - {k_{\text{s}}}^{-} p_4 p_5 \tag{15}$$

Eqs. (10)–(14) are expressions for the molar rates of formation of the different species based on the stoichiometries of the reactions.

$$R_{CH_4} = -R_{\text{r}} \tag{16}$$

$$R_{CO} = R_{\text{r}} - R_{\text{s}} \tag{17}$$

$$R_{H_2O} = -R_{\text{r}} - R_{\text{s}} \tag{18}$$

$$R_{H_2} = 3R_{\text{r}} + R_{\text{s}} \tag{19}$$

$$R_{CO_2} = R_{\text{s}} \tag{20}$$

For boundary conditions, the composition of the fuel gas is known at the interface between the channel and the electrode interface. At the interface between the channel and electrodes, the molar flux rates of all gasses are known. The resulting system of ordinary differential equations is solved using an iterative Newton-Raphson technique. The validation of the mass transfer section of the model is presented in [15]. It is also shown that the variation of Ψ is at least 10 times more effective at influencing the mass transfer in porous electrodes than other microstructure parameters.

3. Results and discussion

3.1. Effect of the structural parameter Ψ

Fig. 2 shows a graph of numerical results of hydrogen concentration at the triple phase boundary (TPB) of a fuel cell anode for different values of the Ψ parameter constant across the anode thickness and two different fuel supplies. The Ψ parameter has a physical interpretation as the ratio of the anode porosity to tortuosity. The interpretation of the parameter is important through much of the paper. A structure with large Ψ can be interpreted as either a high porosity or low tortuosity material. Both of these lead to a decrease in resistance to mass transfer. On the other hand, a low Ψ leads to an increased resistance to mass transfer because the structure has low porosity or high tortuosity.

The current density is set at 500 mA cm^{-2}. Similar trends were observed at other current densities. The fuel for the dotted line is 20% H_2, 3% H_2O, and 77% N_2. For the solid line, the fuel is 20% H_2 with 25% CH_4, 45% H_2O, 7% CO, and 3% CO_2. This figure is an example of the effect electrode microstructure has upon mass transfer within the electrodes. It also illustrates how the incorporation of some amount of internal reforming vastly changes the gas distribution in the anode. The concentrations are measured at the TPB because this is the concentration that changes the operational voltage of a SOFC. Hydrogen at the TPB falls significantly with an increase in Ψ when internal reforming is present. When a diluted hydrogen stream is fed to the fuel cell, the partial pressure of H_2 increases with an increase in the value of the Ψ parameter. This can be explained by the source of H_2 that internal reforming introduces into the system. The longer residence time of CH_4 in the anode microstructure, caused by the lower Ψ value (more tortuous channels), leads to an increase in H_2 production within the electrode volume. These results strongly suggest that microstructural grading of the electrode can improve fuel cell performance.

3.2. Polarization effects

Section 3.1 has shown that electrode microstructure for different fuel compositions has substantial impact on cell performance. This is further shown through polarization curves in Figs. 3 and 4, where graphs of voltage versus current density are given for a variety of constant and graded microstructures. Four cases are presented and used henceforth. Values of Ψ from 0.05 to 0.25 are modeled, approximating minimum and maximum physically realistic values from literature [8,12], respectively. The cases are:

- {1} and {2} are when the Ψ parameter is kept constant at a representative maximum and minimum value (0.05 and 0.25) across the anode thickness, respectively.
- {3} is when the Ψ parameter across the anode thickness is varied linearly from 0.25 at the fuel inlet channel to 0.05 at the electrolyte interface.
- {4} is when the Ψ parameter across the anode thickness is varied linearly from 0.05 at the fuel inlet channel to 0.25 at the electrolyte interface.

The numerical model showed that the resulting cases in between these extreme values of Ψ predictably lie within the results given by these values. Linear grading of SOFC materials has been obtained using advanced ceramic techniques [7]. An electrode can also be composed of layers of constant (psi). In this study, the layers of constant Ψ will be represented as a linear variation along the anode thickness.

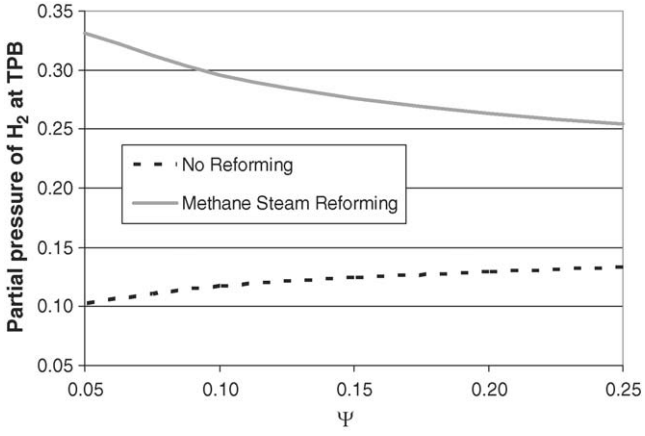

Fig. 2. Numerical predictions of Ψ vs. partial pressure of H_2 at the TPB for a current density of 500 mA cm^{-2}. Results show that this value changes very differently with Ψ depending on fuel composition.

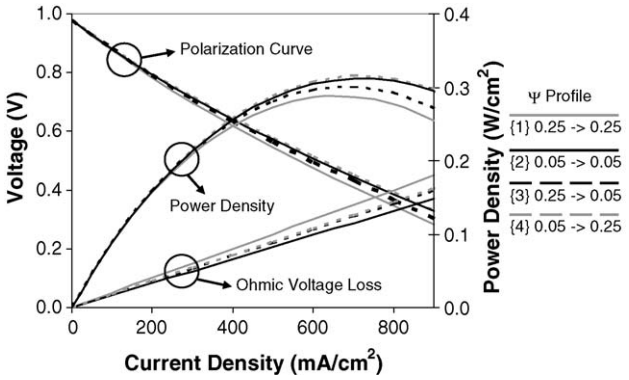

Fig. 3. Total cell voltage for a 20% H_2/3%H_2O/77% N_2 fuel stream with different anode microstructures. Maximum power density is 8.7% higher for case {4} than for case {1}.

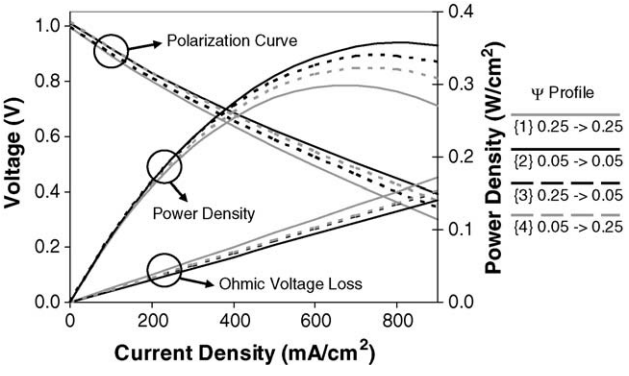

Fig. 4. Total cell voltage for a 20% H_2/25% CH_4/45% H_2O/7% CO/3% CO_2 fuel stream with various alternative anode microstructures. Maximum power density is 19% higher for case {2} than for case {1}.

Table 1
List of parameters used in this study

Parameter	Value
Temperature (T, K)	1273
Pressure (P, atm)	1.00
Exchange current density (i_o, A/cm^2)	0.05
Transfer coefficient (β)	0.5
Anode thickness (L_A, mm)	1.0
Anode bulk resistivity (ρ, Ω/m)	0.001
Anode tortuosity (τ_A)	2.00
Anode pore radius (r, μm)	1.05
Cathode thickness (L_C, μm)	20
Cathode bulk resistivity (p, Ω/m)	3.5
Cathode tortuosity (τ_C)	2.00
Cathode pore radius ($\langle r \rangle$, μm)	0.75
Electrolyte thickness (L_E, μm)	10
Electrolyte resistivity (ρ_E, Ω/m)	0.20

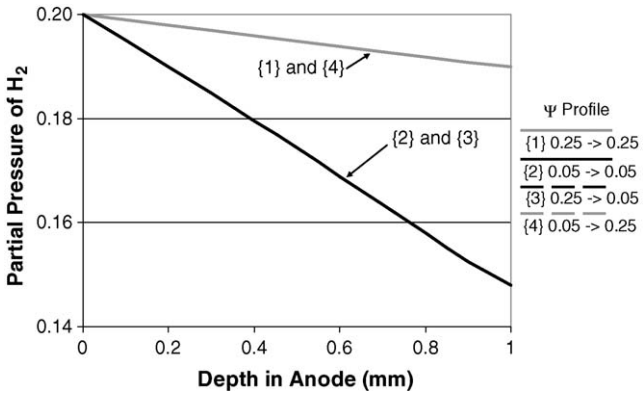

Fig. 5. Hydrogen concentration profiles through the anode thickness for microstructure cases {1}–{4} with diluted hydrogen fuel. The TPB is located at 1 mm depth.

In Fig. 3 the fuel stream provided to the cell is 20% H_2, 3% H_2O, and 77% N_2. Fig. 4 shows an internal reforming SOFC with a 20% H_2, 25% CH_4, 45% H_2O, 7% CO, and 3% CO_2 fuel stream. Other parameters considered in this study are shown in Table 1. With these cases, the effect of grading the microstructure of a SOFC anode upon the actual fuel cell performance is predicted.

In Fig. 3, minimal polarization is observed to occur for case {4}, which has a graded microstructure. Only a slightly better performance is seen for this case than for no microstructure grading (case {2}). The ohmic voltage losses are also shown in this figure. Both electrode grading methods produced a microstructure with the same average resistance, as expected. The lowest ohmic voltage loss is seen for case {2} because low porosity material provides more material for electronic conduction. The worst ohmic voltage loss is seen for the high Ψ electrode {1} due to its high resistance. And the graded electrodes have a performance in between these two constant microstructure cases, and do not reflect the same trend shown in the polarization curve since concentration and activation polarization also plays a role in cell performance. We observed the lowest concentration polarization at maximum power for cases {1} and {4} (results not shown). This can be attributed the high species counter-diffusion flux area at the TPB where H_2O is produced and H_2 is actively consumed, producing large concentration gradients. The open pore structure at the TPB given by the graded electrode allows more effective gas transport while still keeping ohmic losses low. It is important to note that current cell designs have outer layers that are relatively porous with a thin low porosity layer near the TPB. The philosophy behind this is to not limit mass transfer with a thick layer of low porosity material near the channel and to increase the active TPB area. This modeling suggests that alternative electrode structural designs are worth considering. It should also be noted that most functional grading methods have a performance that is minimally lower than a homogeneous electrode for the H_2 fed fuel cell.

Fig. 4 displays the additional effect of internal reforming in the anode. The Nernst voltage was calculated with the values of H_2 and H_2O concentrations at the TPB. The concentration polarization does not have a meaningful reference in this case because, due to internal reforming, the channel concentration of H_2 does not represent a significant value for comparison. The result is markedly different from Fig. 3. The best performance is seen for case {2}, which represents a homogeneous low porosity/high tortuosity structure.

This means that there are limited benefits seen under these operating conditions to justify the extra cost of manufacturing the graded structure. The internal reforming of CH_4 leads to a large increase in H_2 concentration throughout the anode, from 10% at the inlet to typically 30% at the TPB. In fact, the efficiency of this reforming process is a large driver for the performance of the cell. It is also observed that one of the main reasons for the increase in performance for case {2} is that it has the lowest ohmic losses. We observed that the key to the better performance is an effective reforming reaction. If lower levels of reforming are seen, the system will begin to resemble a humidified H_2 fuelled system and performance may be gained by electrode grading. An analysis of the fuel cell operating range would be required to make a decision on the suitability of this scheme.

The effect of changing the cathode porosity was also studied. It was computed that the same variation of the microstructural parameter Ψ as given for cases {1}–{4} above leads to a variation in performance of less than 1%. This is attributed to the lack of counter-diffusion that occurs in this electrode as the oxygen ions are directly transported through the electrolyte. This observation also suggests the possible application of functionally graded electrodes to anionic conducting electrolytes.

3.3. Species diffusion in graded microstructure electrodes

The species within the fuel cell are investigated at 500 mA cm^{-2} current density and conditions described in Table 1. The figures will provide insight into the physical mechanisms that drive the changes in performance that are seen in Figs. 3 and 4. Hydrogen will be the species studied because of its obvious importance to fuel cell performance.

Fig. 5 is a graph of the partial pressure of H_2 throughout the depth of the anode for the four cases of Ψ grading when

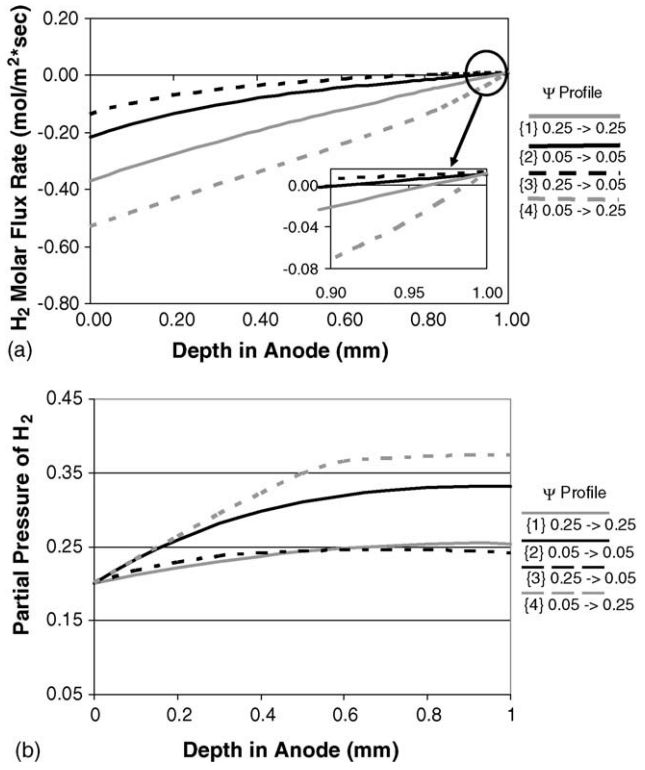

Fig. 6. (a) Hydrogen flux profiles through the anode thickness for microstructure cases {1}–{4} with internal reforming. The TPB is located at 1 mm depth, (b) hydrogen concentration profiles through the anode thickness for microstructure cases {1}–{4} with internal reforming. The TPB is located at 1 mm depth.

the SOFC is fed with diluted H_2 fuel. It is seen that the same concentration profile is predicted for each case where the Ψ value at the TPB is the same. This is evidence of the importance of the TPB upon the mass transfer in a operational SOFC. Because the fuel cell is operating at steady state it can only maintain a linear concentration profile when there are no internal sources of species, as is the case of a diluted hydrogen fuel. This leads to the concentration profile being determined by the largest resistance in the electrode, which is the area at the TPB. A high Ψ value at the TPB enhances mass transfer in this area and therefore increases the concentration of H_2 at the TPB.

Evidence for the effect of counter-diffusion of species can be seen in the H_2 species molar flux profiles that are shown in Fig. 6(a). These cases are all for identical gas inlet conditions described in Table 1 with internal reforming. The molar flux rate of H_2 is shown through the thickness of the anode. The TPB is at a depth of 1 mm. Hydrogen gas is volumetrically produced in the anode from methane and consumed at the TPB. It is generally seen that the flux profile is most strongly dependent upon the Ψ value that occurs near the TPB. The greatest negative values of H_2 flux are seen for case {4}. For case {1}, where there is also the large pore structures near the TPB, the H_2 flux is also significantly more negative. These results once again support the conclusion that an open pore structure near the electrochemically active layer will enhance the counter diffusion of species that must occur in this region.

This phenomena is also visible is the concentration profiles as seen in Fig. 6(b), which shows hydrogen concentration through the anode thickness. This graph shows a significant increase in the H_2 partial pressure for the case where the microstructure is graded from low Ψ at the fuel channel to high Ψ at the electrolyte interface. However, it was shown in Fig. 4 that this increase in electrochemical performance is negated by the reduction in electrical conductivity. Anode materials with increased conductivity could change this balance. It can also be seen in Fig. 6(b) that there are significant changes to the rate of change of hydrogen concentration throughout the microstructure thickness. It is clear that case {4} produces a sharp rise in hydrogen concentration that is triggered by the residence time of CH_4 in the surface of the anode. It appears that this is actually enhanced by the increased mass transfer rate that occurs because of the lowering of the Ψ parameter throughout the anode thickness that allows the counter diffusion of reactants to occur near the TPB. Furthermore, it is noted that the smallest TPB H_2 concentration is created by case {1}, which is also the worst electrical conductor. This leads to its theoretically low performance.

4. Conclusions

The effect of electrode microstructure grading on the performance of a solid oxide fuel cell has been studied. This was performed to determine possible ways that the performance can be improved with a simple design. This goal was accomplished by utilizing a numerical model of the fuel cell electrodes, electrolyte, and gas channel to predict performance for alternative electrode geometries.

It was shown that when diluted H_2 is the fuel stream, grading the electrode from less to more porous towards the TPB, increases performance beyond having a monolith of constant Ψ of either extreme value. Also, it was observed that when the microstructure is graded for an internal reforming fuel cell there are no performance gains when available materials are used. It was observed that higher concentrations of H_2 were seen at the TPB when an optimal microstructure was used for an internal reforming fuel cell, but ohmic losses negated this advantage. A detailed investigation of non-isothermal effects is necessary to determine the interplay of heat and mass transfer, and its effect on electrode grading. The use of an electrode that is graded from high Ψ at the TPB to low Ψ at the supply channel has been shown to be an effective way to promote diffusion mass transfer when diluted hydrogen in introduced as a fuel to a SOFC with a significantly thick anode.

Acknowledgements

Financial support is provided by the Office of Naval Research (ONR) University /Laboratory Initiative (ULI) program. Specifically, thanks are due to Richard Carlin, Michele Anderson, and David Drumheller at ONR and Eric Dow, Maria Medeiros, Alan Burke, Louis Carreiro, Russell Bessette, Craig Deschenes, Steven Tucker, and Delmas Atwater at the Naval Undersea Warfare Center, Newport, RI.

References

[1] H. Kim, S. Park, J.M. Vohs, R.J. Gorte, J. Electrochem. Soc. 148 (2001) A693–A695.
[2] J. Deseure, Y. Bultel, L. Dessemond, E. Siebert, Electrochim. Acta 50 (2005) 2037–2046.
[3] N. Hart, N. Brandon, M. Day, N. Lapena-Rey, J. Power Sources 106 (2002) 42–50.
[4] Y. Liu, C. Compson, M. Liu, J. Power Sources 138 (2004) 194–198.
[5] E. Murray, A. Barnett, Solid State Ionics 143 (2001) 265–273.
[6] E. Muller, C. Drassar, J. Schilz, W. Kaysser, Mater. Sci. Eng. A 362 (2003) 17–39.
[7] C. Gerk, M. Willert-Poada, Mater. Sci. Forum 308–311 (1999) 766–773.
[8] M. Mogensen, N. Sammes, G. Tompsett, Solid State Ionics 129 (2000) 63–94.
[9] T. Kenjo, M. Nishiya, Solid State Ionics 57 (1992) 295–302.
[10] S.H. Chan, Z.T. Xia, J. Power Sources 93 (2001) 130–140.
[11] H. Zhu, R.J. Kee, J. Power Sources 117 (2003) 61–74.
[12] W. Lehnert, J. Meusinger, F. Thom, J. Power Sources 87 (2000) 57–63.
[13] D. Arnost, P. Schneider, Chem. Eng. J. 57 (1995) 91–99.
[14] B. Todd, J.B. Young, J. Power Sources 110 (2002) 186–200.
[15] E.S. Greene, M.G. Medeiros, W.K.S. Chiu, J. Fuel Cell Sci. Technol. 140 (2005) 136–140.